Rheological characterization of ionic liquids and ionic liquid crystals with promising tribological performance†

Tobias Amann,*[a] Christian Dold[a] and Andreas Kailer[a]

Received Xth XXXXXXXXXX 20XX, Accepted Xth XXXXXXXXX 20XX
First published on the web Xth XXXXXXXXXX 200X
DOI: 10.1039/b000000x

Several rheological studies of ionic liquids and ionic liquid crystals were performed to describe the measured low coefficients of friction ($\mu \approx 0.02$) in reciprocating sliding tests (cylinder-on-disc, ring-on-disc). The main mechanisms which are assumed to lead to low friction values are the chemical composition of the anion and the orientation of the molecules under shear. The ionic liquid crystals show strong non-Newtonian viscosity behavior and viscoelastic properties in the liquid crystalline phase. In addition, the viscosity depends on the molecule orientation, which can be influenced by shear. At the transition from the liquid crystalline to the isotropic phase a strong decrease of viscosity is observed.

1 Introduction

Ionic liquids (ILs) are promising fluids for several technical applications and the development of so called room-temperature ionic liquids, thus salts which are already liquid at room-temperature, was a great advancement [1]. An overview of the physical properties and opportunities for possible applications of ILs is given from Wasserscheid and Rogers [2,3]. ILs have also shown good performance as lubricants in tribological applications [1,4]. Because of the many tribological results, which are described in literature, ILs count as versatile and possible novel lubricants [5]. One key property characteristic of ILs, with respect to tribological applications, is their rheological behavior. The rheological behavior of phosphonium-based ILs [6] and of $[C_4mim][NTf_2]$ [7] is already described in literature. In addition, the viscosity under high pressure [8] and influenced by magnetic and electrical fields [9] was investigated. There are many publications which quote the viscosity values for several ILs [10,11]. For example Seddon et al. [12] describe the viscosity and density of 1-alkyl-3-methylimidazolium salts of $[BF_4]^-$, $[PF_6]^-$, $[Cl]^-$, $[CF_3SO_3]^-$ and $[NO_3]^-$. Because of the high amount of possible modifications (10^{12} to 10^{18}) of ILs [13] it is necessary to develop methods to predict their physical properties [14]. It was found, that there is a strong relationship between the viscosity and the molecular volume of ILs [14]. In addition, there have also been some efforts to simulate the rheological behavior of ILs [15]. ILs can also show non-Newtonian viscous shear thinning because of the existence of liquid phase aggregates [16]. Nanorheological studies using surface force apparatus (SFA) experiments showed that two imidazolium-based ILs, which are confined in molecularly thin films between charge-bearing mica surfaces, exhibit molecular layering [17]. This confinement leads to a drastically viscosity increase over several orders of magnitude, whereas the ILs confined between two noncharged methyl-terminated surfaces show no layering [17].

Already before ILs became interesting as a class of special lubricants, liquid crystals were discussed as promising lubricants [18]. Some mesogenic fluids were found that lead to ultralow friction values in reciprocating tribological contacts [19,20]. Concerning the tribological results of liquid crystals and ILs it could be assumed, that ionic liquid crystals (ILCs) are also a promising class of fluids with specific tribological properties. ILCs are able to form liquid crystalline phases because of the distinct anisotropy of the chemical structure of the cation [21]. An overview on the chemical properties of ILCs is given from Axenov and Laschat [22]. In contrast to ILs, ILCs exhibit much higher water content in the neat form, especially when halogenic anions are used such as bromide or chloride. Therefore it is assumed that there are some problems with the corrosivity of the ILCs [23]. So far LCs were only described as lubricant additives in marginal amount to improve the tribological behavior [24,25]. ILCs show also a specific rheological behavior especially in the liquid crystalline phase. For example 1,3-Didodecylimidazolium salts show strong non-Newtonian viscosity behavior in the liquid crystalline state and no shear dependent viscosity in the isotropic phase [26].

Aim of this work is to characterize the rheological behavior of ILs and ILCs and to relate it to their tribological behavior. Therefore the viscosity of different imidazolium-based

† Electronic Supplementary Information (ESI) available: Values of the dynamic viscosities. Yield-stress, frequency sweeps and relaxation measurements. See DOI: 10.1039/b000000x/

[a] *Fraunhofer Institute for Mechanics of Materials IWM, Woehlerstraße 11, 79108 Freiburg, Germany. Fax: +49 7615142-510; Tel: +49 7615142-208; E-mail: tobias.amann@iwm.fraunhofer.de*

ILs was analyzed with respect to the alkyl chain length and the chemical character of the anion. The rheological behavior of ILCs in the liquid crystalline state and in the isotropic phase was compared also. In addition, the viscoelastic properties of the ILCs were qualified and the orientation of the ILC molecules under shear was studied in the mesogenic phase.

2 Motivation

Friction losses in tribological applications reduce the energy efficiency of technical systems. Therefore novel lubricants with minimal friction losses become increasingly interesting because energy can be saved. A possible approach for lubricants with very low coefficients of friction (μ) is the use of special fluids with specific physical properties. With complex fluids such as mesogenic fluids, ionic liquids and ionic liquid crystals in reciprocating sliding tests (test parameters: 50N, 50Hz, 1mm) friction coefficients lower than $\mu \approx 0.02$ were obtained using different tribological standard tests (ring-on-disc; cylinder-on-disc, cylinder is inclined by 10° to the sliding direction; figure 1). The temperature was maintained by heating up the lower disc.

The results showed that the chemical structure of the anion plays an important role concerning the tribological behavior at relative high initial contact pressure (cylinder-on-disc, 130 MPa) and at low contact pressure (ring-on-disc, 0.5 MPa). $[PF_6]$ containing ILs show lower friction values than those with $[(CF_3SO_2)_2N]$ (figure 1a, b). In contrast, a longer alkyl chain of the imidazolium-based ILs leads to friction coefficients that are in the range of standard lubricants like motor oils (SAE10W40, figure 1a). ILCs show a much higher coefficient of friction (COF) in the liquid crystalline phase (90°C) as in the isotropic phase (120°C). The sharp peak of the COF signal at 4.5 h with $[C_{12}mim][Cl]$ can be interpreted as a solid-solid contact at which the asperities of the specimens get into contact. When the contact geometry is changed to flat ring-on-disc geometry, the influence of the molecular structure becomes weaker (figure 1b). In the liquid crystalline phase the coefficient of friction is 0.12 with cylinder-on-disc geometry for $[C_{12}mim][Cl]$ which is in the same range as for $[C_2mim][(CF_3SO_2)_2N]$ (figure 1a). But at low initial contact pressure these two fluids show totally different tribological behavior (figure 1b). At these conditions $[C_{12}mim][Cl]$ attains low friction in contrast to $[C_2mim][(CF_3SO_2)_2N]$. To explain this result a fundamental knowledge of the rheological characteristics of the different fluids is crucial. A detailed description of the tribological studies on ionic liquids and ionic liquid crystals will be published elsewhere[27].

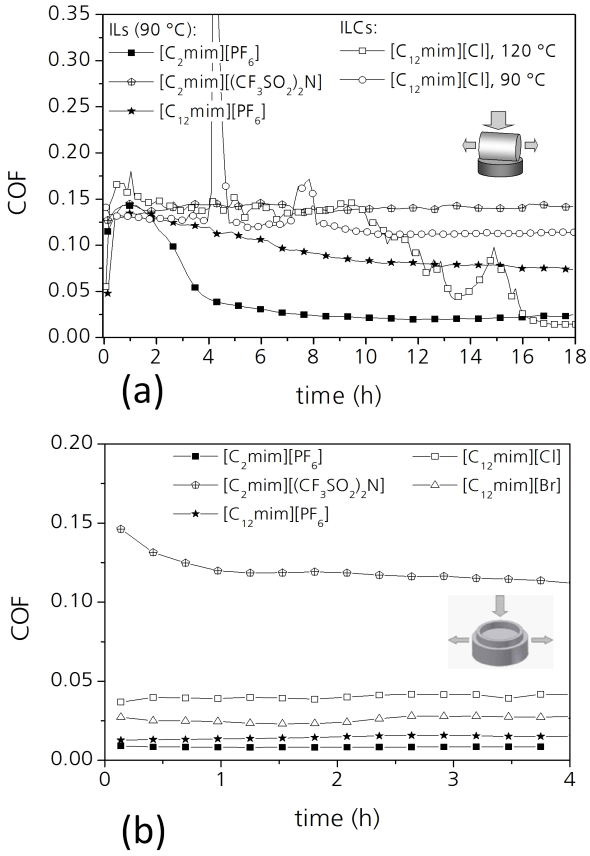

Fig. 1 Coefficient of friction (COF) of the reciprocating friction tests of some selected ionic liquids using two different geometries (50N, 1mm, 50Hz): (a) Cylinder-on-disc test (line contact) at two temperatures for the ILCs (liquid crystalline 90 °C and isotropic 120 °C) for 18 h; (b) Ring-on-disc friction test (surface contact) at 90 °C for 4 h

3 Experimental

3.1 Reagents and Materials

In summary eight different ionic liquids were used, at which two of them were ionic liquid crystals. These two fluids ($[C_{12}mim][Cl]$ and $[C_{12}mim][Br]$) form a smectic-A liquid crystalline phase[28]. In figure 2 the chemical basic structures of the used anions and cations are illustrated.

The acronym R in figure 2a stands for the different alkyl chain lengths. The chemical notation, acronyms, molecular weights, melting points and water contents (manufacturer information) are listed in table 1. The ILs were purchased from Iolitec GmbH.

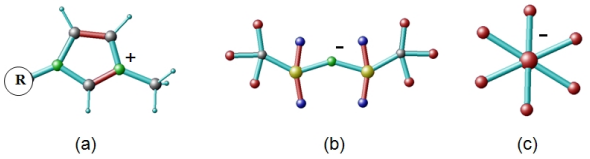

Fig. 2 Chemical basic structure of the used various ions: (a) Methyl-Imidazolium based cation with variable length of the alkyl chain R (red line: double bond; grey atoms: carbon; green atoms: nitrogen); (b) Bis(trifluoromethylsulfonyl)imide anion (red line: double bond; grey atoms: carbon; green atom: nitrogen; blue atoms: oxygen; red atoms: fluorine; yellow atoms: sulfur); (c) Hexafluorophosphate anion (central atom: phosphor; red atoms: fluorine)

Table 1 Disposed ionic liquids for rheological and tribological investigations with their molecular weight (MW), melting point (MP, literature) and water content (WC, manufacturer's data)

Ionic Liquids	MW / $g \cdot mol^{-1}$	MP / °C	WC / ppm
$[C_2mim][PF_6]$	256	62 [29]	140
$[C_2mim][(CF_3SO_2)_2N]$	391	-26 [30]	80
$[C_4mim][PF_6]$	284	11 [29]	160
$[C_8mim][PF_6]$	340	-70 [29]	180
$[C_8mim][(CF_3SO_2)_2N]$	475	-84 [31]	100
$[C_{12}mim][PF_6]$	397	60 [32]	160
$[C_{12}mim][Cl]$	287	109.8 [28]	2560
$[C_{12}mim][Br]$	331	100.2 [28]	3660

3.2 Rheological experiments

Rheological experiments were performed using a modular rotating rheometer (MCR501, Co. Anton-Paar). The EC motor (electronically commutated) equipped with a high-precision air bearing system for minimal friction losses. Rheological tests were conducted in the rotational and oscillatory mode. The standard viscosity measurements were carried out in the rotational mode using a cone-plate system the angle between the surface of the cone and the plate is 2° with a diameter of 50mm (CP50-2/TP). The temperature is maintained over Peltier temperature control by heating the lower plate with an additional Peltier hood to ensure gradient-free measurements. Viscosity curves were measured to characterize the flow behavior with respect to the shear rate. The test procedure was to start at low shear rate ($\dot{\gamma} = 10^{-1}s^{-1}$) and increase the shear rate to $\dot{\gamma} = 10^{3}s^{-1}$. Subsequent the viscosity values were measured at decreasing shear rates from $\dot{\gamma} = 10^{3}s^{-1}$ to $\dot{\gamma} = 10^{-1}s^{-1}$ to analyze time-dependent effects. The viscoelastic properties were measured with the oscillatory mode using the plate-plate configuration (CP50/TP, angular frequency: 10 rad/s , temperature: 90°C, gap: 1.0mm). The dynamic optical rheoanalyzer (DORA) allows the measurement of the flow birefringence (lowest measuring limit: $5x10^{-9}$) and flow dichroism (lowest measuring limit $3x10^{-9}$) at specific shear rates. The accuracy of absolute extinction angle is 0.3° with an extinction angle resolution of 0.01. Polarized light (wave length: 637nm, modulation frequency: 2.2kHz) is used to detect the optical anisotropy induced by shear. DORA consists of a parallel-plate measuring system with a temperature range between 10°C and 70°C. The temperature is maintained by liquid temperature control.

4 Results

4.1 Viscosity values

The rheological tests were performed at 90°C for ILs and at 90°C and 120°C for ILCs. The dynamic viscosities are illustrated in figure 3 at a shear rate of $1000s^{-1}$, because some tested fluids have non-Newtonian flow behavior at low shear rates (viscosity values are listed in ESI†).

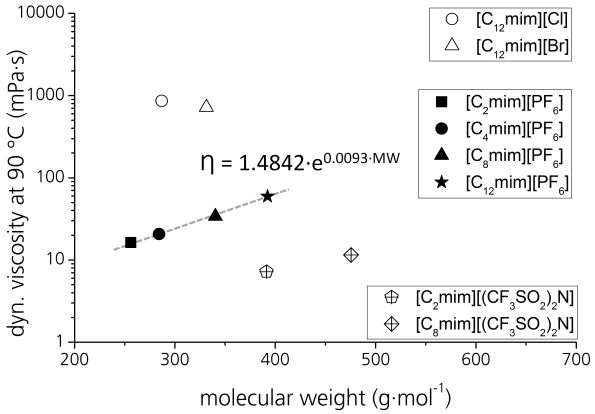

Fig. 3 Viscosity values of the ionic liquids and ionic liquid crystals at high shear rate ($\dot{\gamma} = 1000s^{-1}$, gap: 0.052mm, cone: CP50-2/TP) at 90°C as a function of the molecular weight

The ILCs have by far the highest viscosity and the $[(CF_3SO_2)_2N]^-$ containing ILs the lowest. In relation to $[C_{12}mim][PF_6]$ the two ILCs show much higher viscosity values ($[Cl]^-$: 15-times and $[Br]^-$: 12-times). By changing the anion from $[PF_6]^-$ to $[(CF_3SO_2)_2N]^-$ at the imidazolium-based ILs the viscosity strongly decreases although the molecular weight increases. The viscosity (η) of the four imidazolium-based ILs increases exponentially due to their molecular weight (MW):

$$\eta = 1.4842 \cdot e^{0.0093 \cdot MW} (R^2 = 0.999) \quad (1)$$

Because of the logarithmic plotting the best-fit curve is linear in figure 3. In accordance to these results, Slattery et al. [14] found a strong relationship of the viscosity with the molecular volume and the anion.

4.2 Flow behavior

The flow behavior was analyzed at increasing and, after a break of 60 seconds, decreasing shear rates with a shearing time of 230 seconds. During the break there is no rotation (shear rate = $0s^{-1}$) to give the fluid time for relaxation. The result of the stress relaxation test was, that the resulting shear stress relaxes to a constant value for both ILCs after 60s at a deformation of 10% (figure in ESI†). In the liquid crystalline phase both ILCs show a strong reversible non-Newtonian viscosity behavior (figure 4a). $[C_{12}mim][Br]$ has a higher viscosity than $[C_{12}mim][Cl]$ at low shear rates. The non-Newtonian viscosity character decreases for both fluids in the second half cycle ($\dot{\gamma} = 10^3 s^{-1}$ to $\dot{\gamma} = 10^{-1} s^{-1}$), but there is still non-Newtonian flow behavior.

In the isotropic phase (120 °C) both ILCs show nearly Newtonian flow behavior (figure 4b). Because of the higher melting point of $[C_{12}mim][Cl]$ there is still a marginal shear rate dependence of non-Newtonian flow behavior. At increasing and decreasing shear rates there are nearly no differences in the viscosity values.

$[C_2mim][PF_6]$ shows also a non-Newtonian shear rate dependent flow behavior (4c) but at decreasing shear rates the non-Newtonian flow behavior is less pronounced. This is the only IL of the used ones with a shear rate dependent viscosity.

4.3 Phase transition temperature

The phase transition temperature from liquid crystalline to isotropic was measured with differential scanning calorimetry (DSC). To study the changes of the rheological behavior due to this phase transition the viscosity difference of these two phases was exploited. The temperature dependent viscosities of $[C_{12}mim][Br]$ and $[C_{12}mim][Cl]$ are illustrated in figure 5a. At the phase transition temperature the viscosity decreases suddenly by a factor of 6. The temperatures, at which the viscosity jumps occur, agree well with the transition temperatures measured with DSC (table 2). The transformation enthalpy is higher for $[C_{12}mim][Cl]$ by a factor of 6 (table 2).

Table 2 Comparison of measured phase transition temperature and transformation enthalpy from liquid crystalline to isotropic of the ILCs

Ionic Liquids	Phase transition $(LC-I)$		
	Temperature/°C		Enthalpy / $J \cdot g^{-1}$
	DSC	Rheology	DSC
$[C_{12}mim][Cl]$	115	112	8.13
$[C_{12}mim][Br]$	103	102	1.30

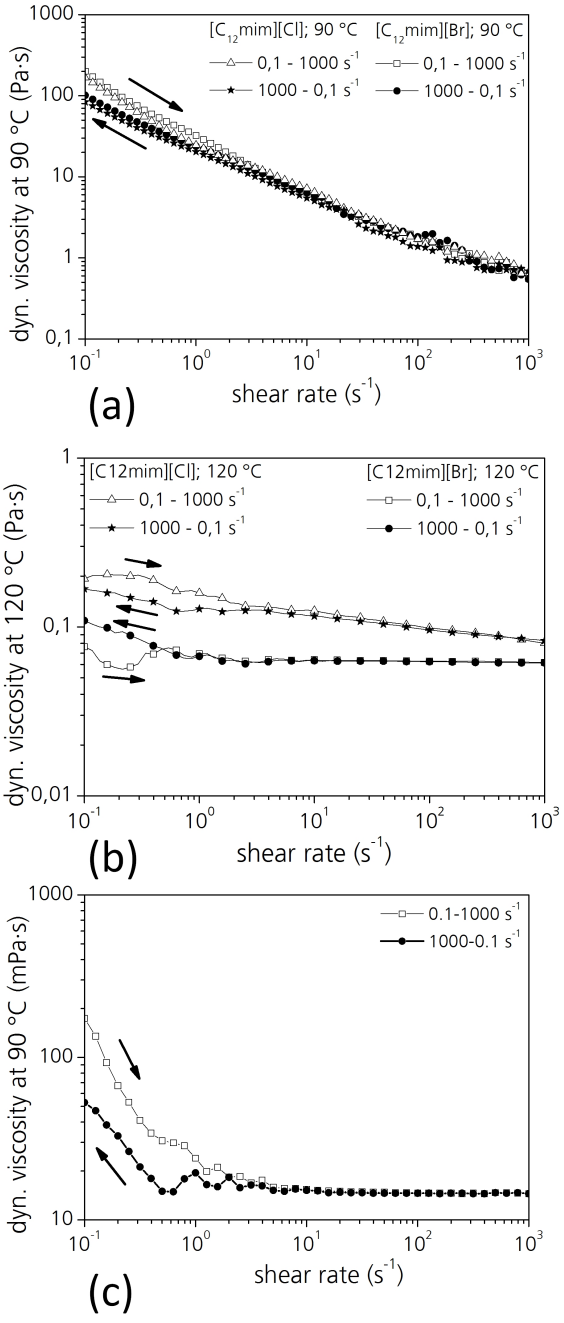

Fig. 4 Viscosity curve by increasing and following decreasing shear rate for (gap: 0.052mm, cone: CP50-2/TP): (a) $[C_{12}mim][Cl]$ and $[C_{12}mim][Br]$ in the liquid crystalline state at 90 °C; (b) $[C_{12}mim][Cl]$ and $[C_{12}mim][Br]$ in the liquid isotropic phase at 120 °C; (c) $[C_2mim][PF_6]$ for two times at 90 °C

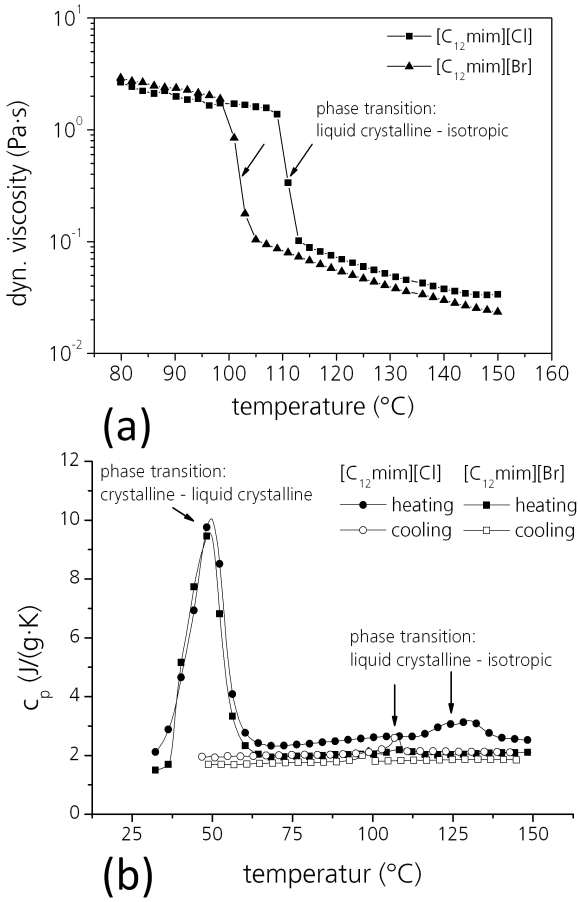

Fig. 5 Determination of the temperature of the transition from the mesogenic to the isotropic phase (LC-I) using two different methods: (a) Measuring the viscosity as a function of the temperature (heating rate: $2\,^{\circ}\mathrm{C}/min$, shear rate: $50s^{-1}$); (b) Differential scanning calorimetry (DSC) with heating rate of $5\,^{\circ}\mathrm{C}/min$ (gap: 0.052mm, cone: CP50-2/TP)

4.4 Viscoelastic properties

To analyze the elastic and viscous characteristics of the fluids rheological tests in the oscillatory mode were performed (angular frequency: 10 rad/s). In addition, the rheological yield point can be determined at the point when the viscous properties exceed the elastic properties. In the liquid crystalline phase the ILCs show a gel character. It was assumed that ILCs show viscoelastic properties in the liquid crystalline phase because of the orientation order of the molecules. In figure 6a the loss modulus and the storage modulus of the two ILCs $[C_{12}mim][Br]$ and $[C_{12}mim][Cl]$ are illustrated as a function of the shear stress.

At small shear stresses both ILCs show linear viscoelasticity with stronger elastic properties, whereas $[C_{12}mim][Cl]$ has

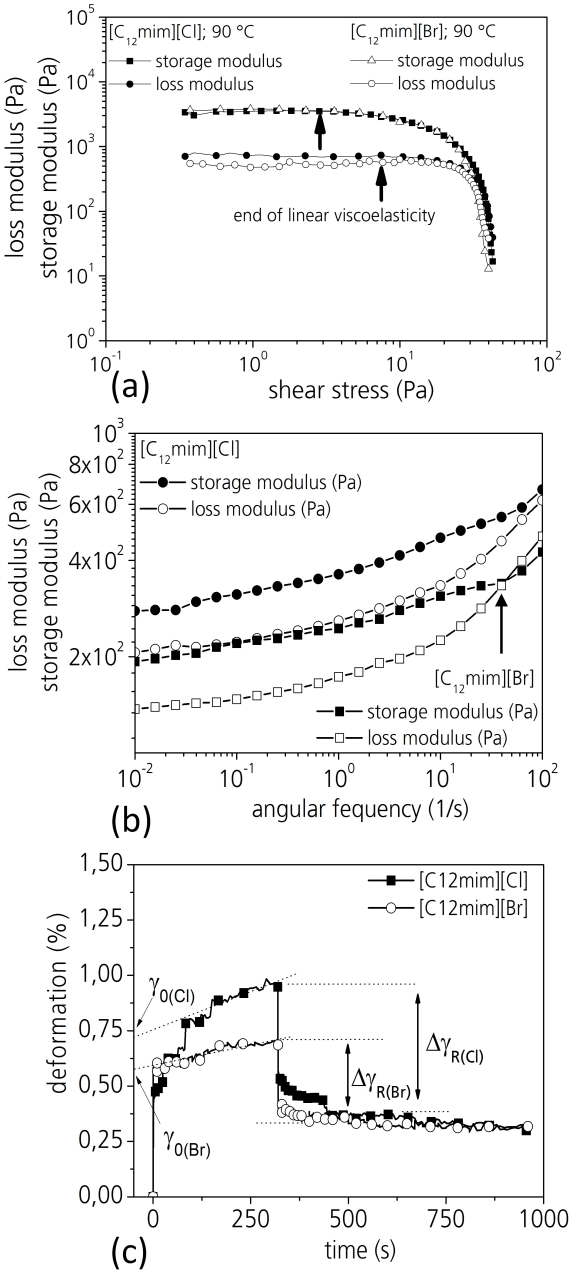

Fig. 6 Rheological characterization of $[C_{12}mim][Cl]$ and $[C_{12}mim][Br]$ (plate-plate configuration at 90 °C and 1.0mm gap): a) Amplitude sweep: Comparison of the yield-stress; b) Frequency sweep at 10% deformation; c) Creep test at constant shear stress of 10 Pa and following creep recovery with 0 Pa

a little higher loss modulus as $[C_{12}mim][Br]$. This linear viscoelastic area ends for both ILCs at a shear stress of approximately 10 Pa because at this point the value of the storage modulus starts to change. Above this shear rate the structured order of the ILCs with viscoelastic properties is destroyed. The yield points, were the storage modulus is similar to the loss modulus, is determined for $[C_{12}mim][Br]$ to 30 Pa and for $[C_{12}mim][Cl]$ to 35 Pa (additional figure in ESI†). It was observed that all tested ILs did not show viscoelastic behavior at 90 °C and also the ILCs exhibit only viscous properties in the isotropic phase (120 °C).

The corresponding frequency sweep is illustrated in figure 6b (deformation: 10%, angular frequency: 0.01 to $100s^{-1}$). The elastic properties are throughout higher for $[C_{12}mim][Cl]$ as the viscous properties. In contrast, $[C_{12}mim][Br]$ shows a point of intersection at an angular frequency of $40s^{-1}$. At lower deformation (1% and 5%, figures in ESI†) the storage modulus is nearly constant and above the loss modulus, which increases with increasing angular frequency.

The creep test was performed to analyze the creep recovery behavior of $[C_{12}mim][Cl]$ and $[C_{12}mim][Br]$ after applying a constant shear stress of 10 Pa for 320s. The deformation is measured which shows a linear increase after a specific time. γ_0 is the elastic and γ_R the reversible deformation. A flow process is an irreversible deformation and therefore the system doesn't relax complete to the initial state. Only the elastic part of the deformation can be recovered and the viscous part dissipates. $[C_{12}mim][Br]$ has an elastic deformation $\gamma_{0(Br)}$ of 0.58% and $[C_{12}mim][Cl]$ of 0.71%. The calculated reversible deformation after 180s creep recovery without shear stress are $\gamma_{R(Br)} = 0.37\%$ and $\gamma_{R(Cl)} = 0.58\%$.

4.5 Orientation effects under dynamic conditions

Due to their ability to form ordered structures liquid crystals are birefringent. This can be explored when the orientation of the molecules under shear are determined. These measurements will then give information about the orientation mechanisms in a tribological contact, but it must be noticed that at tribological contacts the shear rates can be much higher because of the very small gap width. The orientation angle is the average angle which molecules form with respect to the flow direction. This angle was measured at two different shear rates for each fluid to analyze if there is a relation between the orientation angle and the viscosity. The configuration of the test setup was a plate-plate system in rotational mode at 70 °C. Therefore the two ILCs were analyzed in the liquid crystalline phase.

The results for $[C_8mim][PF_6]$ are illustrated in figure 7a. The measured orientation angle is zero during the whole measurement, which indicates that the molecules are all aligned along the flow direction. It must be noticed, that the shear rate of 10^4s^{-1} is very high and there could be some instabilities of the measured values in respect to figure 7a. The viscosity decreases due to shear rate ($\dot{\gamma} = 10^3s^{-1}$ to $\dot{\gamma} = 10^4s^{-1}$) from $0.14mPa \cdot s$ to $0.11mPa \cdot s$.

In the nonoperating state $[C_{12}mim][Cl]$ has an orientation angle of approximately 10° and $[C_{12}mim][Br]$ of 30°. For $[C_{12}mim][Cl]$ the orientation angle changes directly to zero at a shear rate of $\dot{\gamma} = 10^2s^{-1}$, which indicates that already all molecules are orientated along the flow direction (figure 7b). In contrast $[C_{12}mim][Br]$ still shows an orientation angle of approximately 15° at a shear rate of $\dot{\gamma} = 10^2s^{-1}$ (figure 7c). By increasing the shear rate to $\dot{\gamma} = 10^3s^{-1}$ there is also a uniform orientation of the molecules in flow direction. The shear rate increase leads to a decrease of the viscosity value for $[C_{12}mim][Cl]$ from $7Pa \cdot s$ to $1Pa \cdot s$ and in analogy for $[C_{12}mim][Br]$ from $4Pa \cdot s$ to $1Pa \cdot s$.

The corresponding values of flow birefringence (Δn) for the measured orientation angles are shown in figure 8. The results show that all three studied liquids have a positive and high value of Δn in the range of 10^{-5} to 10^{-4}. When the orientation angle is close to zero (i.e. full orientation along the flow) it corresponds to a higher level of molecular ordering which results in higher Δn-values for both ILCs. $[C_{12}mim][Cl]$ shows, in contrast to $[C_{12}mim][Br]$ and $[C_8mim][PF_6]$, constant values of flow birefringence over the testing time. For $[C_{12}mim][Br]$ and $[C_8mim][PF_6]$ the value of flow birefringence is connected to the shear rate, whereas $[C_{12}mim][Br]$ shows a broad scatter band at lower shear rates. By increasing the shear rate from $\dot{\gamma} = 10^2s^{-1}$ to $\dot{\gamma} = 10^3s^{-1}$ Δn increases for $[C_{12}mim][Br]$. $[C_8mim][PF_6]$ shows a contrariwise behavior, because Δn decreases by increasing the shear rate from $\dot{\gamma} = 10^3s^{-1}$ to $\dot{\gamma} = 10^4s^{-1}$. For these both fluids the change of Δn results in a decreasing viscosity value, whereas $[C_{12}mim][Br]$ has a constant Δn-value and viscosity independent of the shear rate.

5 Discussion

The rheological measurements were performed to analyze the relationship between the friction coefficient and rheological properties of different ionic liquids. The tribological measurements showed for imidazolium-based ILs with $[PF_6]^-$ for an alkyl chain length up to 8 carbon atoms low friction coefficients ($\mu \approx 0.02$, 90 °C, cylinder-on-disc) in contrast to ILs with $[(CF_3SO_2)_2N]^-$ ($\mu \approx 0.15$, 90 °C, cylinder-on-disc) as anion (figure 1a). This result is not related to the viscosity values because the ILs with $[(CF_3SO_2)_2N]^-$ show lower viscosities as the comparable ILs with $[PF_6]^-$. For the ILC $[C_{12}mim][Cl]$ even a lower coefficient of friction ($\mu \approx$ 0.1, 120 °C, cylinder-on-disc) was measured although it had the highest viscosity of all tested fluids. $[C_{12}mim][Cl]$ and $[C_{12}mim][Br]$ have a 12-times higher viscosity at 90 °C than $[C_{12}mim][PF_6]$ because $[C_{12}mim][PF_6]$ exhibits no liquid crys-

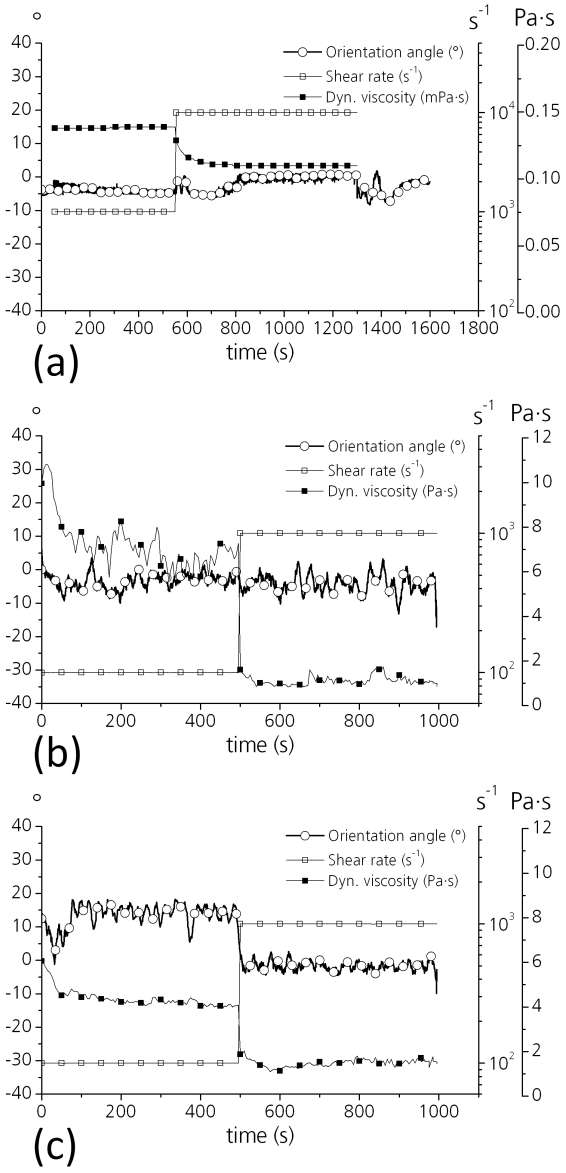

Fig. 7 The measuring of the average orientation angle of the molecules in the liquid crystalline phase in respect to the shear rate at 70 °C with the dynamic optical rheo-analyzer for three different fluids (configuration: plate-plate, material: glass, gap: 0.5mm): (a) $[C_8mim][PF_6]$; (b) $[C_{12}mim][Cl]$; (c) $[C_{12}mim][Br]$

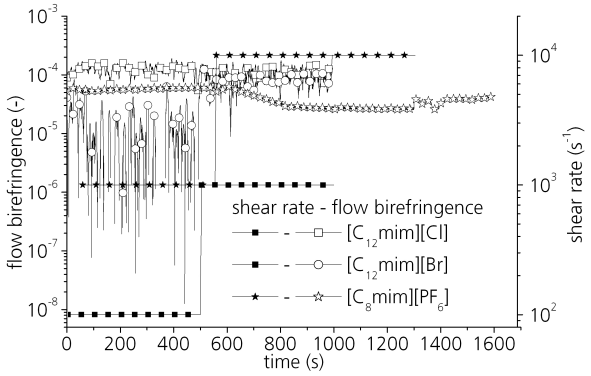

Fig. 8 Measured values of the flow birefringence related to the shear rate according to figure 7 (open symbols: flow birefringence; filled symbols: shear rate)

talline phase[21]. In the liquid crystalline phase, with highly ordered structures, $[C_{12}mim][Cl]$ gains a much higher friction value of $\mu \approx 0.12$.

There is a correlation between the molecular weight respectively to the alkyl chain length of the cation and the viscosity within ILs with the same chemical composition. The increase within the imidazolium-based ILs with $[PF_6]^-$ shows an exponential dependency due to the molecular weight. The increasing viscosity is assumed to be the reason for the increasing running-in phase, until low friction is reached.

Friction tests with lower initial contact pressure (ring-on-disc) however showed that also $[C_{12}mim][Cl]$ in the liquid crystalline phase and $[C_{12}mim][PF_6]$ can achieve low friction values (figure 1b). This contradiction of measured low coefficient of friction (ring-on-disc) despite high viscosity led to the assumption, that ionic liquids have lower viscosity values at high shear rates and moderate contact pressure. The viscosity measurements at different shear rates indicate that the viscosity decreases at higher shear rates. Optical analysis showed that the molecules of $[C_8mim][PF_6]$ and $[C_{12}mim][Cl]$ are uniformly aligned along the flow direction already at lower shear rates as the molecules of $[C_{12}mim][Br]$.

These results show, that the macroscopic measured viscosity is not the essential material property for the tribological performance for this testing setup. The viscosity affects the duration of the running-in period, and therefore wear mechanisms at the beginning of the test, but not the absolute value of the coefficient of friction. Therefore it is assumed that chemical interactions play an important role for the tribological behavior of ILs. In addition, it must be noticed that the rheological properties can be also affected by other mechanisms in the tribo contact. Because of the confinement and therefore the thin film lubrication, there are much higher shear rates which can influence the rheological behavior of the fluid [17]. But these mechanisms have to be analyzed using other

techniques like SFA (surface force apparatus) or in-situ IR-spectroscopy. Therefore it is not possible to estimate what viscosity is required to achieve the best tribology result.

The reversible shear rate dependent viscosity of the ILCs in the liquid crystalline state indicates that there is shear thinning due to orientation effects of the molecules, which doesn't arise in the isotropic phase. Due to the optical analysis it is assumed that this non-Newtonian flow behavior in the liquid crystalline phase arises from a reorientation of the molecules. The nature of the flow behavior of $[C_2mim][PF_6]$ may not be connected to shear thinning or orientation of the molecules. The non-reversible shear rate dependency could arise because of wettability of $[C_2mim][PF_6]$ with the solid surface of the fixture. These intermolecular interactions between the steel plate and the IL get maybe destroyed due to shear.

In addition, it is shown, that the ILCs exhibit viscoelastic behavior with a defined yield point in contrast to ILs in the liquid crystalline phase. We assume that the higher COF at ring-on-disc geometry for $[C_{12}mim][Cl]$ is caused by the higher loss modulus and the higher yield point of $[C_{12}mim][Cl]$ compared to $[C_{12}mim][Br]$. We also showed, that at the phase transition temperature the viscosity of the ILCs strongly changes with the breakdown of the molecular alignment in the isotropic phase. $[C_{12}mim][Cl]$ shows a higher phase transition enthalpy which indicates that it has a more ordered liquid crystalline structure as $[C_{12}mim][Br]$. More ordered LC structure of $[C_{12}mim][Cl]$ can be seen from the higher Δn-values in figure 8. This could be the reason for the higher viscosity of $[C_{12}mim][Cl]$ at 90°C despite the lower molecular weight, which causes the higher COF for $[C_{12}mim][Cl]$ for the ring-on-disc geometry.

6 Conclusions

The rheological behavior of ionic liquids and ionic liquid crystals were investigated to understand the mechanisms which cause low friction values. In reciprocating sliding tests (cylinder-on-disc, ring-on-disc) with ionic liquids and ionic liquid crystals friction coefficients lower than $\mu \approx 0.02$ were obtained. In particular orientation effects of the molecules due to shear were explored and correlated with the viscosity values.

The main mechanisms to realize low friction values are assumed to be the chemical composition of the anion and the orientation of the molecules under shear. These both factors affect the viscosity value and the interaction of the liquid with the surface. The chemical interaction of the ionic liquid and the surface strongly influences the tribological behavior because low viscosities are not related to low friction values. In addition, the viscosity of ionic liquid crystals is connected to the orientation of the molecules, which can be influenced by shear stress. This indicates that there could be strong viscosity changes under tribological conditions for ionic liquid crystals because of the high shear rates at tribological contacts.

Within a chemical similar group of ionic liquids the viscosity increases with molecular weight. At higher viscosity the running-in time increases. For the imidazolium-based ILs with $[PF_6]^-$ there is an exponential dependency of the viscosity in respect to the molecular weight. In accordance it was found that the irreversible non-Newtonian flow behavior of $[C_2mim][PF_6]$ is connected to the interaction of the IL with the surface (wettability). In contrast the reversible non-Newtonian flow behavior in the liquid crystalline phase for the ionic liquid crystals arises due to shear thinning because of orientation of the molecules. At the transition temperature from the liquid crystalline to the isotropic phase the viscosity strongly decreases and the viscoelastic properties disappear.

Acknowledgments

The authors gratefully acknowledge the DFG priority program SPP 1191 (KA2745/3-1) for financial support of this work.

References

1 M.-D. Bermúdez, A.-E. Jiménez, J. Sanes and F.-J. Carrión, *Molecules*, 2009, **14**, 2888–2908.
2 P. Wasserscheid and T. Welton, *Ionic liquids in synthesis*, Wiley-VCH, Weinheim, 2nd edn, 2007, vol. 2, p. 724.
3 R. D. Rogers and K. R. Seddon, *Ionic Liquids III A: Fundamentals, Progress, Challenges, and Opportunities*, American Chemical Society, Washington, DC, 2005.
4 I. Minami, *Molecules*, 2009, **14**, 2286–2305.
5 C. Ye, W. Liu, Y. Chen and L. Yu, *Chem. Commun.*, 2001, **21**, 2244–2245.
6 M. D. Green, C. Schreiner and T. E. Long, *J. Phys. Chem. A*, 2011, **115**, 13829–13835.
7 H. Chen, Y. He, J. Zhu, H. Alias, Y. Ding, P. Nancarrow, C. Hardacre, D. Rooney and C. Tan, *International Journal of Heat and Fluid Flow*, 2008, **29**, 149–155.
8 A. Pensado, M. Comunas and J. Fernandez, *Tribology Letters*, 2008-08-01, **31**, 107–118.
9 A. Bicak, H. T. Belek and A. Göksenli, *Acta Polytechnica*, 2005, **45**, 68–72.
10 J. Jacquemin, P. Husson, A. A. H. Padua and V. Majer, *Green Chem.*, 2006, **8**, 172–180.
11 D. R. MacFarlane, J. Golding, S. Forsyth, M. Forsyth and G. B. Deacon, *Chem. Commun.*, 2001, **16**, 1430–1431.
12 R. K. Seddon, A. Stark and M.-J. Torres, *ACS Symposium Series*, American Chemical Society, 2002, vol. 819, pp. 34–49.
13 A. R. Katritzky, R. Jain, A. Lomaka, R. Petrukhin, M. Karelson, A. E. Visser and R. D. Rogers, *J. Chem. Inf. Comput. Sci.*, 2002, **42**, 225–231.
14 J. M. Slattery, C. Daguenet, P. Dyson, T. J. S. Schubert and I. Krossing, *Angewandte Chemie*, 2007, **119**, 5480–5484.
15 N. V. Pogodina, M. Nowak, J. Lauger, C. O. Klein, M. Wilhelm and C. Friedrich, *Journal of Rheology*, 2011, **55**, 241–256.
16 G. L. Burrell, N. F. Dunlop and F. Separovic, *Soft Matter*, 2010, **6**, 2080–2086.
17 I. Bou-Malham and L. Bureau, *Soft Matter*, 2010, **6**, 4062–4065.
18 F.-J. Carrión, G. Martínez-Nicolás, P. Iglesias, J. Sanes and M.-D.

Bermúdez, *International Journal of Molecular Sciences*, 2009, **10**, 4102–4115.
19 T. Amann and A. Kailer, *Tribology Letters*, 2011, **41**, 121–129.
20 T. Amann and A. Kailer, *Tribology Letters*, 2010, **37**, 343–352.
21 K. Binnemans, *Chemical Reviews*, 2005, **105**, 4148–4204.
22 K. V. Axenov and S. Laschat, *Materials*, 2011, **4**, 206–259.
23 K. R. Seddon, A. Stark and M.-J. Torres, *Pure Appl. Chem*, 2000, **72**, 2275–2287.
24 C. Zhang, S. Zhang, L. Yu, P. Zhang, Z. Zhang and Z. Wu, *Tribology Letters*, 2012, 1–6.
25 P. G.Iglesias, M. Bermúdez, F. Carrión and G. Martínez-Nicolás, *Wear*, 2004, **256**, 386–392.
26 X. Wang, F. W. Heinemann, M. Yang, B. U. Melcher, M. Fekete, A.-V. Mudring, P. Wasserscheid and K. Meyer, *Chem. Commun.*, 2009, **47**, 7405–7407.
27 T. Amann, C. Dold and A. Kailer, *Tribological behavior of complex fluids with low friction values: mesogenic fluids, ionic liquids and ionic liquid crystals, in prep.*
28 A. Getsis, *PhD thesis*, University Köln, 2008.
29 I. López-Martin, E. Burello, P. N. Davey, K. R. Seddon and G. Rothenberg, *ChemPhysChem*, 2007, **8**, 690–695.
30 A. R. Choudhury, N. Winterton, A. Steiner, A. I. Cooper and K. A. Johnson, *CrystEngComm*, 2006, **8**, 742–745.
31 D. Almantariotis, T. Gefflaut, A. A. H. Pádua, J.-Y. Coxam and M. F. Costa Gomes, *The Journal of Physical Chemistry B*, 2010, **114**, 3608–3617.
32 C. M. Gordon, J. D. Holbrey, A. R. Kennedy and K. R. Seddon, *J. Mater. Chem.*, 1998, **8**, 2627–2636.